Published in final edited form as:
Mol Microbiol. 2012 November ; 86(4): 954–970. doi:10.1111/mmi.12035.

LuxU Connects Quorum Sensing to Biofilm Formation in *Vibrio fischeri*

Valerie A. Ray and **Karen L. Visick***
Department of Microbiology and Immunology Loyola University Medical Center Maywood, IL

Summary

Biofilm formation by *Vibrio fischeri* is a complex process involving multiple regulators, including the sensor kinase (SK) RscS and the response regulator (RR) SypG, which control the symbiosis polysaccharide (*syp*) locus. To identify other regulators of biofilm formation in *V. fischeri*, we screened a transposon library for mutants defective in wrinkled colony formation. We identified LuxQ as a positive regulator of *syp*-dependent biofilm formation. LuxQ is a member of the Lux phosphorelay and is predicted to control bioluminescence in concert with the SK AinR, the phosphotransferase LuxU, and the RR LuxO. Of these, LuxU was the only other regulator that exerted a substantial impact on biofilm formation. We propose a model in which the Lux pathway branches at LuxU to control both bioluminescence and biofilm formation. Furthermore, our evidence suggests that LuxU functions to regulate *syp* transcription, likely by controlling SypG activity. Finally, we found that, in contrast to its predicted function, the SK AinR has little impact on bioluminescence under our conditions. Thus, this study reveals a novel connection between the Lux and Syp pathways in *V. fischeri*, and furthers our understanding of how the Lux pathway regulates bioluminescence in this organism.

Keywords

Vibrio fischeri; biofilm; quorum sensing; phosphorelay; sensor kinase; phosphotransferase

Introduction

Bacteria readily adapt to changing environmental conditions by sensing and integrating different cues present in their surroundings to produce a response appropriate for survival or growth. One mechanism by which bacteria coordinate such responses is through the use of two-component systems, with the sensor kinase (SK) component involved in detecting and relaying an environmental cue, and the response regulator (RR) component promoting the response, often a change in gene expression (Stock *et al.*, 2000, West & Stock, 2001). A classic example of signal integration via two-component regulators is the Lux pathway in the marine bioluminescent bacterium *Vibrio harveyi* (Ng & Bassler, 2009). This organism integrates distinct signals (small molecules termed autoinducers or AIs) using specific SKs that funnel their activities into a common phosphorelay pathway to control the production of cellular bioluminescence.

In *V. harveyi*, the Lux pathway (Fig. 1A) is composed of the SKs LuxQ (in association with the periplasmic protein LuxP), LuxN, and CqsS (not depicted), the histidine phosphotransferase LuxU, and the RR LuxO (reviewed in (Ng & Bassler, 2009)). Under low cell densities (low AI concentrations), the SKs exhibit net kinase activity and serve as

*Corresponding author: Mailing address: Karen L. Visick, 2160 S. First Ave. Bldg. 105, Rm. 3933, Department of Microbiology and Immunology, Loyola University Medical Center, Maywood, IL 60153, (708) 216-0869, (708) 216-0869 (Fax), kvisick@lumc.edu.

phosphoryl-donors to LuxU, which serves as a phosphoryl-donor to the RR LuxO. Phosphorylated LuxO (LuxO~P) then promotes the transcription of five sRNAs (*qrr1-5*), which bind to and destabilize (in conjunction with Hfq) the transcript for the master transcriptional regulator $LuxR_{VH}$. This regulator promotes the transcription of the *lux* operon, which encodes the proteins necessary for light production. Without $LuxR_{VH}$, light is not produced. However, as the cell density increases, the AI concentrations also increase, causing a shift in the equilibrium of SK activity (i.e., from net kinase to net phosphatase activity). This switch to net phosphatase activity promotes the removal of phosphoryl groups from LuxO through LuxU. Without LuxO~P, $LuxR_{VH}$ is produced and promotes the expression of the *lux* operon, ultimately leading to light production.

Similar pathways exist in a variety of other *Vibrio* species, including *V. parahemolyticus, V. cholerae*, *V. anguillarum*, *V. vulnificus*, and *V. fischeri* (Milton, 2006, Zhang *et al.*, 2012). Like *V. harveyi*, the *V. fischeri* Lux pathway also controls bioluminescence (reviewed in (Stabb *et al.*, 2008, Miyashiro & Ruby, 2012)). The *V. fischeri* Lux components appear similar to those in *V harveyi* (Fig. 1). For example, *V. fischeri* encodes (or is predicted to encode) homologs of LuxP, LuxQ, LuxU, and LuxO, which are proposed to function in a manner similar to their counterparts in *V. harveyi* (Miyamoto *et al.*, 2000, Visick, 2005, Stabb *et al.*, 2008, Miyashiro *et al.*, 2010); however, differences between the Lux pathways in *V. fischeri* and *V. harveyi* exist. For example, *V. fischeri* does not encode a homolog of CqsS or LuxN, but encodes another sensor kinase, AinR, predicted to function at the same level as LuxQ (Gilson *et al.*, 1995, Stabb *et al.*, 2008, Miyashiro & Ruby, 2012). Furthermore, LuxO~P controls the transcription of a single *qrr* sRNA, which likely binds to and destabilizes the transcript of the transcriptional regulator LitR (a $LuxR_{VH}$ homolog) (Miyamoto *et al.*, 2003, Miyashiro *et al.*, 2010). Finally, LitR controls the transcription of an additional downstream regulator, $LuxR_{VF}$ (not similar to $LuxR_{VH}$) (Fidopiastis *et al.*, 2002), which activates the *lux* operon when bound by its AI (Stevens *et al.*, 1994, Sitnikov *et al.*, 1995). Thus, *V. fischeri* integrates AI cues to not only regulate the phosphorylation state of the RR LuxO, but also to regulate the transcription of the *lux* operon, adding another level of control to the production of cellular bioluminescence in this organism.

In addition to controlling bioluminescence, the Lux pathway in *V. fischeri* impacts other processes such as acetate metabolism (Studer *et al.*, 2008) and motility (Lupp & Ruby, 2005, Hussa *et al.*, 2007, Cao *et al.*, 2012). Lux regulates a variety of processes in other *Vibrios* as well. For example, *V. cholerae, V. anguillarum, V. vulnificus,* and *V. parahaemolyticus* utilize the Lux pathway to control biofilm formation via regulators downstream of LuxO (Croxatto *et al.*, 2002, Hammer & Bassler, 2003, Enos-Berlage *et al.*, 2005, Lee *et al.*, 2007, Zhang *et al.*, 2012). For *V. fischeri*, no clear connection between the Lux pathway and biofilm formation has been observed, with the exception that a *litR* mutant exhibits a change in colony morphology (from translucent to opaque) consistent with a possible alteration in biofilm formation (Fidopiastis *et al.*, 2002). Thus, it seems likely that *V. fischeri* could utilize the Lux pathway to regulate biofilm formation, but the exact role, if any, has yet to be determined.

V. fischeri is known to promote biofilm formation through the symbiotic polysaccharide (*syp*) locus (Fig. 1B). The *syp* locus is set of 18 genes thought to be involved in the regulation, production, and transport of a polysaccharide involved in biofilm formation (Yip *et al.*, 2005, Yip *et al.*, 2006, Shibata & Visick, 2012). This locus is transcriptionally controlled by the RR SypG, encoded within the *syp* locus, and σ^{54} (Yip *et al.*, 2005). Another regulator of the *syp* locus is the SK RscS, which functions upstream of SypG to promote *syp* transcription (Yip *et al.*, 2006, Hussa *et al.*, 2008). Under standard laboratory conditions, *V. fischeri* does not form robust biofilms (i.e., wrinkled colony formation and pellicle production). However, robust biofilms that are dependent on the *syp* locus can be

induced by overexpression of either *rscS* (Yip *et al.*, 2006) or *sypG*; for SypG to induce biofilm formation, the biofilm inhibitor protein SypE must be absent or inactivated (Hussa *et al.*, 2008, Morris *et al.*, 2011). This enhanced biofilm production correlates with a competitive advantage for colonization by *V. fischeri* of its symbiotic host, the squid *Euprymna scolopes* (Yip *et al.*, 2006, Morris *et al.*, 2011).

In the current study, we sought to identify other components involved in biofilm formation by *V. fischeri* and found that the Lux pathway plays a role in this phenotype. Regulation of biofilm formation by the Lux pathway in *V. fischeri* is novel, as LuxU plays an important role but LuxO involvement is minimal. Our data indicate that the Lux pathway in *V. fischeri* branches at LuxU to regulate both bioluminescence and *syp*-dependent biofilm formation. Additionally, we have evidence to suggest that the SK AinR plays a minimal role in regulating light production and no role in regulating biofilm formation, under our conditions. Thus, this work provides new insight into the mechanism by which the Lux pathway functions in *V fischeri*, and also helps further our understanding of the complex regulatory network involved in controlling biofilm formation in this organism.

Results

Transposon mutagenesis reveals a regulatory connection between syp and lux

To better understand the requirements for biofilm formation in *V. fischeri*, we performed a random transposon mutagenesis of KV3299, a strain that lacks the *syp* biofilm inhibitor protein SypE. We then induced biofilm formation by introducing the *sypG* overexpression plasmid pEAH73; under these biofilm-inducing conditions, *V. fischeri* forms wrinkled colonies instead of smooth colonies (Hussa *et al.*, 2008). We screened approximately 5000 mutants for those exhibiting a defect in wrinkled colony formation and found 27 that appeared to form smooth colonies. To verify the phenotypes of these mutants, we cured them of their *sypG* overexpression plasmid and then re-introduced it. All of the mutants remained defective in wrinkled colony formation and fell into two classes. Class 1 mutants (24 total) exhibited smooth colony morphology (compare Fig. 2A and B), while class 2 mutants (3 total) exhibited a substantial delay (approximately 6 h) in the start of wrinkled colony formation, but appeared similar to that of the parent strain at later times (compare Fig. 2A and C; asterisks indicate the time at which wrinkled colony formation is apparent, typically identified by ridge formation around the outer edge of the spot). To further evaluate these mutants, we performed Southern blot analysis on each mutant to determine whether the transposon had inserted within the *syp* locus, a location predicted to disrupt wrinkling. We found that the class 1 (smooth) mutants mapped within this locus, while the class 2 (delayed) mutants were unaltered in their *syp* regions (data not shown). These results confirm the assumption that wrinkled colony formation induced by *sypG* overexpression depends on the *syp* locus. Because our goal was to identify novel (non-*syp*) factors involved in biofilm formation, we pursued characterization of the class 2 mutants. Upon cloning and sequencing the DNA flanking the site of the Tn insertion in each class 2 mutant, we found that one insertion mapped near the end of *VF_0707*, while the other two were within *VF_0708* (Fig. 2D). These genes are predicted to encode LuxP and LuxQ, respectively, two proteins proposed to be involved in controlling bioluminescence in *V. fischeri* (Fig. 1B).

Loss of LuxQ affects bioluminescence and biofilm formation

In *V. fischeri*, LuxP and LuxQ are predicted to regulate bioluminescence due to their sequence similarity to the well-characterized proteins of *V. harveyi* (58% and 44% identical, 72% and 67% similar, respectively) and to the functional conservation of other members of the *lux* regulatory pathway between *V. harveyi* and *V. fischeri* (reviewed in (Stabb *et al.*, 2008)); however, the functions (bioluminescence or otherwise) of these two proteins in *V.*

fischeri have not yet been assessed through mutagenesis studies. Thus, to understand the functions of these putative regulators, we asked whether these genes were involved in controlling bioluminescence, in addition to probing their role in controlling biofilm formation. Since the Tn insertions were in a Δ*sypE* background, it was first necessary to ask whether loss of SypE impacted luminescence; we found that it did not substantially impact luminescence (Fig. S1A), regardless of whether we used OD_{600} to estimate cell number (Fig. S1B) or determined the number of colony forming units (CFU) (Fig. S1C) to calculate the specific luminescence. Next, we assessed the impact of the Tn mutations on luminescence. The model (Fig. 1B), generated from work in *V. harveyi* (Bassler *et al.*, 1994, Neiditch *et al.*, 2005), predicts that a *luxP* mutant should fail to transmit the AI signal to LuxQ, causing LuxQ to remain a kinase; as a result, the levels of LuxO~P should be higher and luminescence should be lower. The model also predicts that the *luxQ* mutant should exhibit a decrease in LuxO~P levels, leading to increased luminescence. We found that all three mutants exhibited an increase in luminescence relative to their parent (Δ*sypE*) (Fig. 3A).

Since the *luxP* Tn mutant did not exhibit the predicted luminescence phenotype, we hypothesized that the Tn insertion, which was located at the end of *luxP*, was polar on *luxQ*. To test this prediction, we constructed in-frame deletions of both *luxP* (Δ*luxP*) and *luxQ* (Δ*luxQ*) in both the Δ*sypE* and wild-type backgrounds. Neither mutation impacted growth of *V. fischeri* (data not shown). Regardless of the background, loss of LuxP decreased bioluminescence, while loss of LuxQ increased bioluminescence as predicted (Fig. 3B and data not shown). The luminescence of the Δ*luxQ* mutant could be restored to the level of the $luxQ^+$ control by expression of an epitope-tagged version of *luxQ* (*luxQ-FLAG*) in single copy from the chromosome (Fig. 3C). Together, these data indicate that: 1) LuxP and LuxQ are involved in controlling bioluminescence, as predicted, 2) the Tn insertion within *luxP* was polar on *luxQ*, and 3) *luxP* and *luxQ* likely comprise an operon (Fig. 2D).

Since the Tn insertion in *luxP* was polar on *luxQ*, we predicted that the 6 h delay in biofilm formation initially observed from the Tn mutants was likely due to loss or disruption of *luxQ*. To test this prediction, we examined wrinkled colony formation by the Δ*luxQ* (Δ*sypE*) mutant that overexpressed *sypG*. Like the Tn mutants, loss of LuxQ resulted in a similar delay in biofilm formation relative to the control (compare Fig. 4A & B). This delay in biofilm formation could be complemented by expression of *luxQ-FLAG* in single copy from the chromosome of the Δ*luxQ* mutant (Fig. 4A–C). Thus, LuxQ appears to control both bioluminescence and biofilm formation in *V. fischeri*. In contrast, the *luxP* mutation exerted relatively little effect on biofilm formation (Fig. S2); thus, we focused our subsequent studies on LuxQ and other Lux regulators.

LuxU exerts a more substantial impact on biofilm formation than LuxO

In *V. harveyi*, LuxQ functions through the phosphotransferase LuxU, to control the phosphorylation state of the RR LuxO (Fig. 1A) (Freeman & Bassler, 1999b, Freeman & Bassler, 1999a). Since LuxQ is involved in controlling biofilm formation in *V. fischeri,* we asked whether LuxU and LuxO were also involved. Thus, we generated deletions of both *luxU* (Δ*luxU*) and *luxO* (Δ*luxO*) in the Δ*sypE* background. However, it was necessary to first confirm that our mutants exhibited the predicted pattern of luminescence [i.e., increased bioluminescence; for *luxO* mutants, this has been previously reported (Lupp *et al.*, 2003, Hussa *et al.*, 2007)] (Fig. 1B). As expected, both mutants exhibited an increase in bioluminescence relative to their parent (Fig. 3D and Fig. S1). Neither mutant exhibited a growth defect (data not shown). Finally, a Δ*luxU* Δ*luxO* (Δ*sypE*) mutant exhibited a luminescence phenotype similar to that of the individual mutants (Fig. 3D). Overall, these data confirm that *luxU* functions to control bioluminescence in *V. fischeri*, as predicted.

Next, we introduced the *sypG* plasmid into the Δ*luxU* and Δ*luxO* mutants and assessed wrinkled colony formation. Similar to the loss of LuxQ, loss of LuxU resulted in a delay (about 7 h) in wrinkled colony formation (compare Fig. 5A & B). However, loss of LuxO resulted in only a slight, but reproducible delay (1.5 h) in wrinkled colony formation (compare Fig. 5A and C); we also observed the same slight delay for a *luxO::kan* mutant (data not shown), confirming the results of the Δ*luxO* mutant. These data suggest that, under our conditions, LuxU plays a more critical role than LuxO in controlling biofilm formation. These results also suggest that LuxU may function independently of LuxO to control biofilm formation. To investigate this possibility further, we evaluated biofilm formation by the Δ*luxO* Δ*luxU* (Δ*sypE*) mutant. We predicted that if LuxU functions through LuxO to regulate biofilm formation, then loss of both LuxU and LuxO would result in a phenotype similar to loss of LuxO alone (i.e., a 1.5 h delay). This was not the case: loss of both regulators resulted in an 8 h delay in wrinkled colony formation (compare Fig. 5A and D). This delay supports the hypothesis that the two regulators function independently to impact biofilm formation. Furthermore, this result contrasts with the luminescence results, in which the phenotypes of the *luxU*, *luxO*, and *luxU luxO* mutants were similar (Fig. 3D), and which suggest that LuxU likely functions through LuxO to control bioluminescence. Together, these data suggest that the Lux pathway branches at LuxU to control both bioluminescence and biofilm formation (Fig. 1B). Since loss of LuxU resulted in a more severe biofilm phenotype than loss of LuxO, we chose to pursue the role of LuxU (and its inputs) in the current study.

LuxQ kinase activity promotes biofilm formation

Our current data suggest that LuxQ functions as a positive regulator of biofilm formation under our conditions. Because this SK is predicted to function as both a kinase and a phosphatase (Freeman & Bassler, 1999a, Neiditch *et al.*, 2006), we asked whether the ability of LuxQ to positively regulate biofilm formation depended upon its kinase and/or phosphatase activity. Previous work from *V. harveyi* had demonstrated that certain point mutations cause the loss of one activity but not the other (i.e., kinase activity is lost, while phosphatase activity is retained and vice versa) (Neiditch *et al.*, 2006). Thus, we generated point mutations in the *V. fischeri luxQ* gene that are predicted to cause either loss of phosphatase activity (*luxQ-A216P*; kin+/phos−) or loss of kinase activity (*luxQ-H378A*; kin −/phos+), while retaining the other activity, respectively. We then expressed these *luxQ* alleles in single copy from the chromosome of the Δ*luxQ* mutant. To confirm that these LuxQ derivatives were functional, we examined their ability to control light production. According to the model (Fig. 1B) and work from *V. harveyi* (Neiditch *et al.*, 2006), a phosphatase mutant (LuxQ-A216P, kin+/phos−) should exhibit a decrease in bioluminescence (due to an increase in LuxO~P), while a kinase mutant (LuxQ-H378A, kin −/phos+) should exhibit an increase in bioluminescence (due to a decrease in LuxO~P). Indeed, each mutant exhibited the expected pattern of luminescence (Fig. 3C), indicating that the proteins produced were functional and behaved as predicted.

We next assessed the ability of these alleles to complement the Δ*luxQ* mutant with respect to the timing of wrinkled colony formation. We found that the phosphatase mutant, LuxQ-A216P (kin+/phos−), could complement the *luxQ* mutant, restoring the timing of wrinkled colony formation to approximately that of the control strain (*luxQ*$^{+}$) and the wild-type-complemented Δ*luxQ* mutant (compare Fig. 4A, C, and D). In contrast, the kinase mutant, LuxQ-H378A (kin−/phos+), failed to complement the *luxQ* mutant; this strain exhibited wrinkled colony formation that was indistinguishable from the Δ*luxQ* parent (compare Fig. 4A, B, and E). These data suggest that the kinase activity of LuxQ, but not its phosphatase activity, is necessary to regulate biofilm formation.

The impact of LuxQ on biofilm formation depends on LuxU

Our data indicate that LuxQ (specifically its kinase activity) and LuxU are necessary to regulate biofilm formation. According to the model (Fig. 1B), LuxQ is predicted to function through LuxU. To test this hypothesis, we first asked whether LuxQ functioned through LuxU to regulate bioluminescence. If this were the case, we would expect that a *luxQ luxU* mutant would phenocopy a *luxU* mutant, and indeed it did (Fig. 3B). To further evaluate this regulatory connection, we expressed the *luxQ-A216P* (kin+/phos−) allele in the *luxQ luxU* mutant. Whereas, in the context of the *luxQ* (*luxU*$^+$) background this allele decreased luminescence, it failed to do so when *luxU* was also disrupted: the levels of luminescence produced by the *luxQ luxU* mutant expressing *luxQ-A216P* (kin+/phos−) were indistinguishable from that of the *luxU* mutant (Fig. 6A). These data suggest that LuxQ functions through LuxU to regulate bioluminescence.

Next, we asked whether LuxQ functioned through LuxU to control biofilm formation. We first evaluated biofilm formation by the *luxQ luxU* (*sypE*) mutant. We found that the double mutant exhibited a delay in wrinkled colony formation similar to that seen with the individual *luxQ* and *luxU* mutants (Fig. S3), rather than an additive delay. Thus, these results suggest that LuxQ and LuxU function in the same pathway to regulate biofilm formation. To probe this relationship further, we utilized the *luxQ-A216P* allele, which permits complementation of the *luxQ* mutation (Fig. 4). We hypothesized that if LuxU were necessary for LuxQ to regulate biofilm formation, then disruption of *luxU* in the *luxQ* mutant expressing *luxQ-A216P* should delay biofilm formation relative to the *luxU*$^+$ strain. Indeed, this was the case (Fig. 6B). These data suggest that the ability of LuxQ to positively regulate biofilm formation depends upon LuxU.

Biofilm formation depends on the conserved site of phosphorylation in LuxU

In *V. harveyi*, LuxU serves as a phosphotransferase, shuttling phosphoryl groups between the SKs and the RR LuxO (Fig. 1A). This role depends upon the conserved site of phosphorylation, His58 (Freeman & Bassler, 1999b). To determine whether the *V. fischeri* homolog functions in a similar manner, we first constructed an epitope-tagged version of *luxU* (*luxU-FLAG*). Expression of this allele in single copy from the chromosome of the Δ*luxU* mutant restored luminescence to that of the control (Fig. 3E), as well as the normal timing of wrinkled colony formation (compare Fig. 7A–C). Next, we substituted the predicted, conserved histidine for an alanine (H61A) in the *luxU-FLAG* construct and introduced this allele into the chromosome of the Δ*luxU* mutant. The Δ*luxU* mutant expressing the *luxU-H61A* allele failed to restore luminescence to the level of the parent (Fig. 3E) and exhibited the same 6 h delay in wrinkled colony formation as the uncomplemented Δ*luxU* mutant (compare Fig. 7B and D). To ensure that the lack of complementation was not due to a reduction or loss of the protein, we performed western blot analysis and found that protein was expressed from both alleles (Fig. S4). Together, these data suggest that the conserved site of phosphorylation in LuxU is necessary to regulate biofilm formation. Thus, it appears that key residues predicted to be involved in phosphotransfer are required for regulation of biofilm formation.

Loss of AinR has little impact on bioluminescence and no impact on biofilm formation

It has been predicted that, like the *V. harveyi* Lux pathway, multiple SKs feed into LuxU to control bioluminescence in *V. fischeri* (Visick, 2005, Stabb *et al.*, 2008, Miyashiro & Ruby, 2012). In particular, the SK AinR is proposed to function at the same level as LuxQ to control bioluminescence in *V. fischeri* (Fig. 1B) (Gilson *et al.*, 1995, Stabb *et al.*, 2008). To determine whether AinR is involved in controlling bioluminescence and biofilm formation, we generated a Δ*ainR* (Δ*sypE*) mutant and first assessed its luminescence phenotype; no study of AinR has assessed its role in controlling bioluminescence in liquid culture. The

model (Fig. 1B) predicts that, similar to loss of LuxQ, loss of AinR would result in an increase in luminescence. However, this was not the case: loss of AinR resulted in a consistent but very slight decrease in luminescence as compared to the control (Fig. 3F and Fig. S5). To determine whether AinR functioned through the known phosphorelay pathway (i.e., through LuxU), we generated a Δ*ainR* Δ*luxU* (Δ*sypE*) mutant and assessed its luminescence phenotype. We expected that the double mutant would exhibit the luminescence phenotype of the *luxU* single mutant. Surprisingly, this mutant consistently resulted in an intermediate luminescence phenotype: the Δ*ainR* Δ*luxU* mutant was brighter than the Δ*ainR* mutant, but not as bright as the Δ*luxU* mutant (Fig. 3F). These data suggested that AinR may play only a minor role in controlling bioluminescence under these conditions.

As a putative SK, AinR is predicted to recognize and respond to the autoinducer (AI) N-octanoyl-homoserine lactone (C8-HSL) (Gilson *et al.*, 1995). Thus, the diminished luminescence phenotypes of the Δ*ainR* and Δ*ainR* Δ*luxU* mutants could result from a failure of this mutant to respond to C8-HSL. Alternatively, deletion of *ainR* could impact expression of the upstream gene *ainS*, which encodes the C8-HSL synthase protein. An impact on AinS synthesis could lead to decreased amounts of C8-HSL and decreased light production, potentially via direct control of the *lux* operon, as previously demonstrated (Kuo *et al.*, 1996, Egland & Greenberg, 2000). To distinguish between these possibilities, we added exogenous C8-HSL to the *ainR* mutants and controls. We predicted that, if the former hypothesis were true, the *ainR* mutants would retain diminished luminescence relative to their controls. This appeared not to be the case, however, as addition of C8-HSL to the Δ*ainR* and Δ*ainR* Δ*luxU* mutants increased their luminescence levels to those of the control strain and the Δ*luxU* mutant, respectively (Fig. S5B). These data suggest that the decrease in luminescence by both the Δ*ainR* and Δ*ainR* Δ*luxU* mutants is likely due to decreased levels of C8-HSL, whose activity in promoting luminescence is largely or fully independent of the function of AinR, at least under our conditions. Thus, the role of AinR in controlling luminescence remains unclear.

Although AinR did not function as predicted in controlling bioluminescence, we wondered whether loss of AinR would impact biofilm formation. This was not the case: the *ainR* mutant exhibited no defect in biofilm formation, while the Δ*ainR* Δ*luxU* mutant exhibited the defect of the *luxU* mutant (Fig. S6) and could be complemented when the wild-type allele of *luxU-FLAG* was expressed in single copy from the chromosome (data not shown). Thus, AinR has no impact on biofilm formation, and its role in controlling bioluminescence remains unclear. Further work will be necessary to determine what role AinR plays, if any, in controlling luminescence in *V. fischeri*.

LuxU, but not RscS, is necessary to regulate syp-dependent biofilm formation under SypG-inducing conditions

Since the only known role of LuxU is to serve as a phosphoryl-donor (Freeman & Bassler, 1999b, Shikuma *et al.*, 2009) and LuxU impacts *syp*-dependent biofilm formation, we hypothesized that it could function upstream of SypG, a RR known to be required for transcription of the *syp* locus (Yip *et al.*, 2005). Since previous studies had demonstrated that the SK RscS functions upstream of the RR SypG to control *syp*-dependent biofilm formation (Fig. 1B) (Yip *et al.*, 2006, Hussa *et al.*, 2008), we questioned the relative importance of these two potential inputs, RscS and LuxU, on SypG-induced biofilm formation. We thus generated *sypE* mutants with deletions in *luxU*, *rscS*, or both and evaluated SypG-induced biofilm formation. Surprisingly, only loss of LuxU exerted an impact: whereas the *luxU* mutant exhibited a delay in wrinkled colony formation (compare Fig. 8A and C), the *rscS* mutant showed no significant defect in biofilm formation under these conditions (compare Fig. 8A and B). Even when the *rscS* and *luxU* mutations were

combined, this mutant exhibited the same delay as the *luxU* mutant alone could be complemented when the wild-type allele of *luxU-FLAG* was expressed in single copy from the chromosome (compare Fig. 8C and D and data not shown). Overall, these data indicate that LuxU plays a more important role than RscS in controlling biofilm formation when *sypG* is overexpressed.

LuxU functions at or above SypG to impact syp transcription

Since LuxU is necessary to promote *syp*-dependent biofilm formation, we sought to determine whether LuxU functioned upstream of SypG to control its activation (phosphorylation). If so, then we would expect that a phosphorylation-independent allele of SypG would be "blind" to the presence or absence of LuxU. We thus overexpressed a version of SypG in which the conserved site of phosphorylation, D53, was substituted for a glutamate (D53E). This substitution in RRs has previously been shown to promote the active state of the RR (Sanders *et al.*, 1989, Sanders *et al.*, 1992, Freeman & Bassler, 1999a). Indeed, this substitution in SypG caused an increase in SypG activity, as measured by *syp* transcription (Hussa *et al.*, 2008). Consistent with this increased activity, when overexpressed in the Δ*sypE* mutant, *sypG-D53E* induced wrinkling sooner than when the wild-type allele of *sypG* was overexpressed (9–10 h vs. 13–15 h, respectively). When *sypG-D53E* was overexpressed in the Δ*luxU*Δ*sypE* mutant, the timing of wrinkled colony formation was not delayed, but rather was similar to that of the *luxU*$^+$ control (Fig. 9A). These data are consistent with a model in which LuxU functions at or above the level of SypG.

It remains formally possible that the accelerated wrinkling effects of the *sypG-D53E* allele, combined with the delayed wrinkling caused by the loss of LuxU, results in a strain with a net timing of biofilm formation similar to the wild-type strain. Thus, to further probe the level at which LuxU exerts its impact on biofilm formation, we asked whether loss of LuxU affected transcription of the SypG-controlled *sypA* gene using a *lacZ* reporter fusion. We assayed β-galactosidase activity from the reporter expressed from the chromosomes of the Δ*luxU* and the *luxU*$^+$ strains that overexpressed the wild-type allele of *sypG*. Loss of LuxU resulted in a decrease in *syp* transcription at two time points tested (12 and 24 h) (Fig. 9B). Thus, these data suggest that LuxU functions at or above the level of *syp* transcription, potentially due to an impact on SypG activation (Fig. 1B).

Discussion

In this study, we identified a novel connection between the Lux pathway and biofilm formation in *V. fischeri*. Specifically, we found that disruption of either the gene encoding the SK LuxQ or the gene encoding the phosphotransferase LuxU caused a delay in SypG-induced biofilm formation. Surprisingly, this effect was independent of LuxO, which exerted only a minor impact on biofilm formation. However, LuxU does seem to function through LuxO to regulate bioluminescence. Thus, the Lux pathway appears to branch at LuxU to regulate bioluminescence through LuxO and biofilm formation via a SypG-dependent pathway.

From the data presented in this work, we propose a model in which LuxQ functions through LuxU to regulate *syp*-dependent biofilm formation through activation of the RR SypG (Fig. 1B). Support for the idea that LuxQ and LuxU serve as phosphoryl-donors to a downstream regulator of biofilm formation is as follows: 1) the kinase activity of LuxQ is necessary to promote biofilm formation, 2) the predicted, conserved site of phosphorylation in LuxU is necessary to regulate biofilm formation, 3) the only known role of LuxU in the literature is as a histidine phosphotransferase (HPt) (Freeman & Bassler, 1999b, Shikuma *et al.*, 2009), 4) LuxQ depends on LuxU to regulate biofilm formation, and 5) the downstream RR of the

Lux pathway, LuxO, is not required for the effect of LuxU on biofilm formation. Together, these data suggest that phosphotransfer is necessary for LuxQ and LuxU to regulate biofilm formation via a regulator distinct from LuxO. In support of the idea that LuxU serves as an input to regulate the activity of the RR SypG, we found that: 1) a "constitutively active" allele of SypG overcomes the requirement for LuxU, and 2) LuxU functions at or above the level of *syp* transcription. Overall, these data suggest that LuxU functions at or above the level of SypG, potentially at the level of SypG phosphorylation. This possibility is further supported by the fact that SypG and LuxO have similar domain structures (both are σ^{54}-dependent RRs) and exhibit 50% identity to each other. However, proof of such a possibility awaits additional biochemical experimentation; to date, attempts to examine the phosphorylation state of SypG have been unsuccessful. Thus, while our data support the hypothesis that LuxU could serve as a phosphoryl-donor to SypG, the regulation is clearly complex and may include currently unknown regulators.

It has been previously proposed, in two other *Vibrio* species, that LuxU can function independently of LuxO to control the activity of downstream targets of the Lux pathway. The first example is from the fish pathogen *Vibrio anguillarum*. In this organism, VanU functions through VanO to regulate the expression of the $LuxR_{VH}$ homolog, VanT, by activating expression of *qrr1-4* (Croxatto *et al.*, 2004). VanU also appears to act through a VanO-independent mechanism to inhibit the expression of *qrr1-4* (Croxatto *et al.*, 2004, Weber *et al.*, 2011). Weber et al. (2011) thus hypothesize that VanU functions through another RR to repress expression of *qrr1-4*. Similarly, in *Vibrio alginolyticus*, Liu et al (2011) propose that LuxU functions, at least in part, independently of LuxO to control expression of a downstream regulator, LuxT, likely through another RR. However, in neither case has a downstream RR been identified.

There are at least a couple of examples in the literature in which a single domain HPt protein interacts with more than one target RR. *Caulobacter crescentus* ChpT is one such example. ChpT phosphorylates the RRs CtrA and CpdR with equal affinity *in vitro* (Biondi *et al.*, 2006); these phosphorylation events are critical during cell cycle progression. Phosphorylation of CtrA activates this protein, permitting it to bind DNA and control, among other things, DNA replication (Domian *et al.*, 1997, Quon *et al.*, 1998, Jacobs *et al.*, 2003). In contrast, it is the unphosphorylated form of CpdR that is active; in this state, CpdR indirectly promotes degradation of (unphosphorylated) CtrA (Iniesta *et al.*, 2006), permitting the cell to replicate its DNA. Thus, the same phosphorelay controls two separate RRs to exert opposite effects on protein activity.

Another well-studied example of an HPt protein interacting with two RRs occurs in the yeast *Saccharomyces cerevisiae*. In this organism, the HPt protein YPD1 serves as a phosphoryl-donor to the RRs SSK1 and SKN7 under hypo-osmotic conditions (Li *et al.*, 1998). However, YPD1 interacts differently with each RR. For example YPD1 stabilizes the phosphorylated state of the RR SSK1 via protein-protein interactions, but does not form stable complexes with the RR SNK1 (Janiak-Spens *et al.*, 2000). Phosphorylation of SSK1 inactivates this regulator until the cell experiences hyperosmotic conditions, in which case SSK1 is rapidly dephosphorylated and activates a downstream pathway involved in controlling osmotic stress genes (Posas *et al.*, 1996, Posas & Saito, 1998). In contrast, phosphorylation of SNK1 promotes activation of a downstream pathway involved in controlling genes for the cell wall and cell cycle (Morgan *et al.*, 1995, Li *et al.*, 1998, Bouquin *et al.*, 1999). These activities of YPD1 allow for the coordinated regulation of multiple pathways in *S. cerevisiae*. It is possible that LuxU similarly provides a mechanism for coordination of two distinct pathways in *V. fischeri*.

One question that remains is why only the kinase activity of LuxQ, but not its phosphatase activity, is important for biofilm formation. Furthermore, making LuxQ a "constitutive" kinase through three predicted routes (LuxQ-A216P mutation, deletion of *luxP*, or deletion of *luxS*) did not (reproducibly, in the case of LuxQ-A216P) promote accelerated biofilm formation by *V. fischeri* (Fig. 4D, Fig. S2, and Ray and Visick, unpublished data). Potentially, similar to the yeast system described above, LuxU could interact differently with LuxO and SypG, serving as a phosphoryl-donor to both, but only removing the phosphoryl groups from LuxO. Additional work is necessary to better understand the role of the Lux pathway in influencing biofilm formation.

Our work provides insight into the control of biofilm formation by *V. fischeri*, but also challenges the current model of how the Lux pathway regulates bioluminescence in *V. fischeri*. While LuxP, LuxQ, LuxU, and LuxO appeared to function to regulate bioluminescence as predicted (or as previously shown for LuxO (Miyamoto *et al.*, 2000)) (Figs. 1B & 3B and D), the SK AinR did not. Loss of AinR led to a slight decrease in luminescence compared to the control strain (Fig. 3F and S5), while loss of both AinR and LuxU resulted in an intermediate level of luminescence compared to the *ainR* and *luxU* mutants (Fig. 3F). However, the decreased luminescence of the *ainR* and *ainR luxU* mutants could be overcome by the addition of exogenous C8-HSL, which is normally produced by the AI synthase AinS. From these data, we conclude that deletion of *ainR* impacts expression of the gene encoding *ainS* (located directly upstream of *ainR*), and that loss of AinR itself has little impact on bioluminescence. Furthermore, it seems possible that AinR may not function through the known phosphorelay, or at least not through LuxU, to control bioluminescence. These data are not inconsistent with those reported by Lyell et al., who showed that, on solid media, loss of AinS resulted in an increased luminescence phenotype that did not depend on AinR function (Lyell *et al.*, 2010). Thus, additional work is necessary to understand what role AinR may have in controlling this process in *V. fischeri*.

If AinR doesn't function through the known phosphorelay to regulate bioluminescence, does LuxQ serve as the only input? Our data suggest that this is not the case: loss of LuxU resulted in a greater increase in luminescence than loss of LuxQ (Fig. 3B). In both *V. cholerae* and *V. harveyi*, three SKs feed into LuxU (LuxQ, CqsS, and VpsS, and LuxQ, LuxN, and CqsS, respectively) (Ng & Bassler, 2009). In *V. fischeri*, no gene for CqsS exists, but one for VpsS is present (Shikuma *et al.*, 2009). Thus, it is possible that VpsS may also feed into LuxU and serve as another input to regulate light production and possibly biofilm formation. Identifying a missing SK(s) would be an interesting future direction.

This is the first study to examine the role of RscS in biofilm formation under SypG-inducing conditions (overexpression of *sypG* in a Δ*sypE* background). Previous studies have already demonstrated that RscS functions upstream of SypG to induce *syp* transcription in a manner that depends on *sypG* (Hussa *et al.*, 2008) and that RscS is critical in symbiotic biofilm (aggregate) formation and colonization (Visick & Skoufos, 2001, Yip *et al.*, 2006); these previous studies have only explored how loss or overexpression of *rscS* impacts biofilm formation or how its loss impacts colonization. Our findings here indicate that LuxU is more important than RscS for biofilm formation under the conditions we used here. In contrast to these results, our preliminary data for the impact of a *luxU* mutation on the ability of *V. fischeri* to colonize squid revealed, at most, a mild defect due to loss of LuxU (Ray and Visick, unpublished data). These data suggest, perhaps not surprisingly, that our biofilm-inducing (*sypG* overexpression) conditions do not fully reflect the dynamics in nature (during colonization). It is of interest to note, however, that not all symbiosis-competent strains of *V. fischeri* encode a functional RscS protein (Mandel *et al.*, 2009, Gyllborg *et al.*, 2012). Therefore, it is not unreasonable to imagine that another pathway such as Lux could contribute to *syp* induction and biofilm formation during colonization. This work thus

provides an important framework for deepening our understanding of the complex regulatory control over processes critical to colonization by *V. fischeri*.

Experimental Procedures

Bacterial strains and media

V. fischeri strains utilized in this study are shown in Table 1. Strains used in this study were derived from strain ES114, a bacterial isolate from *Euprymna scolopes* (Boettcher & Ruby, 1990). For routine culturing, *V. fischeri* strains were grown in LBS medium (Graf *et al.*, 1994). For luminescence studies, *V. fischeri* strains were grown in Sea Water Tryptone (SWT) (Yip *et al.*, 2005) and SWTO (Bose *et al.*, 2007). All derivatives of *V. fischeri* were generated via conjugation, as previously described (DeLoney *et al.*, 2002). *E. coli* strains GT115 (InvivoGen, San Diego, CA), Tam1 λ pir (Active Motif, Carlsbad, CA), β3914 (Le Roux *et al.*, 2007), π3813 (Le Roux *et al.*, 2007), and CC118 (Herrero *et al.*, 1990) were used for cloning and conjugation. All *E. coli* strains were grown in Luria-Bertani (LB) medium (Davis *et al.*, 1980). Solid media were made using agar to a final concentration of 1.5%. Antibiotics were added to cultures when appropriate to the following final concentrations: ampicillin (Ap) at 100 μg ml^{-1} (*E. coli*), tetracycline (Tet) at 15 μg ml^{-1} (*E. coli*) or 5 μg ml^{-1} (*V. fischeri*), chloramphenicol (Cm) at 20 or 25 μg ml^{-1} (*E. coli*) or 5 μg ml^{-1} (*V. fischeri*), kanamycin (Kan) at 50 μg ml^{-1} (*E. coli*) or 100 μg ml^{-1} (*V. fischeri*), and erythromycin (Erm) at 5 μg ml^{-1} (*V. fischeri*). Along with any necessary antibiotics, diaminopimelate (DAP) was added to a final concentration of 0.3 mM for *E. coli* strain β3914 and thymidine was added to a final concentration of 0.3 mM for *E. coli* strain π3813.

Transposon mutagenesis and identification of mutants with wrinkling defects

Transposon mutants were generated as described previously (Lyell *et al.*, 2008). Briefly, plasmid pEVS170, containing the mini-Tn*5* transposon, was introduced into *V. fischeri* strain KV3299 via conjugation. Ex-conjugates were then pooled and the *sypG* overexpression plasmid pEAH73 was introduced via conjugation. The resultant ex-conjugates were then screened for their ability to form wrinkled colonies. Any mutants found to be defective for wrinkled colony formation after 2 days were then cured of their *sypG* overexpression plasmid and the plasmid was re-introduced. Any mutant that still exhibited a defect was subject to further analysis as described below.

Southern blot analysis

Southern blot analysis was performed as described previously (Visick & Skoufos, 2001, Yip *et al.*, 2005), except chromosomal DNA was digested with KpnI and probed for the *syp* locus or with PstI and probed for Tn sequences. All Tn mutants exhibited a pattern consistent with only one Tn insertion.

Molecular techniques

All plasmids were constructed using standard molecular biological techniques, with restriction and modification enzymes obtained from New England Biolabs (Beverly, MA) or Fermentas (Glen Burnie, MD). Plasmids utilized in this study are shown in Table 2. To identify the site of insertion of the 3 non-*syp* Tn mutants, we cloned the Tn, with flanking DNA, as previously described (Lyell *et al.*, 2008). Unmarked deletions in *V. fischeri* were generated as previously described (Le Roux *et al.*, 2007, Shibata & Visick, 2012). *V. fischeri* ES114 was used as the template in PCR amplifications to obtain the DNA containing or flanking the genes of interest using primers listed in Table S1. PCR products were cloned into the pJET1.2 cloning vector (Fermentas, Glen Burine, MD) or pCR1.2-TOPO (Life Technologies, Grand Island, NY), then subcloned into appropriate final vectors

using standard molecular techniques. Site-directed mutagenesis was performed using the QuikChange Site-Directed Mutagenesis Kit (Stratagene, La Jolla, CA). For complementation in single copy from the chromosome, *luxQ* and *luxU* alleles were cloned upstream of a P_{lacZ} promoter in the mini-Tn*7* delivery vector pEVS107. Insertion at the Tn*7* site of the chromosome was performed via tetraparental mating, as previously described (McCann *et al.*, 2003). All plasmids constructed in this study were sequenced at the Genomics Core Facility at the Center for Genetic Medicine at Northwestern University (Chicago, IL) or ACGT (Wheeling, IL) to ensure that the insertion contained the desired sequence or mutation.

Luminescence assays

V. fischeri cultures were grown in SWT overnight at 24°C with shaking, then diluted to an optical density at 600 nm (OD_{600}) of ~0.01 in 30 ml of SWTO and incubated at 24°C with vigorous shaking. Samples were taken every 30–60 minutes. At each time point, bioluminescence (using a Turner Designs TD-20/20 luminometer at the factory settings and a large, clear scintillation vial) and OD_{600} (using a cuvette) were measured for each sample. Maximum luminescence was observed at OD_{600} measurements between 1.5 and 2 for all strains. Specific luminescence was calculated as relative luminescence (the relative light units of 1 ml of culture integrated over a 6-second count) divided by the OD_{600}.

Wrinkled colony assays

V. fischeri strains were cultured overnight at 28°C with shaking in LBS containing Tet, then sub-cultured 1:100 into fresh LBS containing Tet and grown under the same conditions for 3 to 4 h the next day. Sub-cultures were standardized to an OD_{600} of 0.2 and 10 μl aliquots were spotted onto LBS agar plates containing Tet and incubated at 28°C. Spotted cultures were then monitored from the time the start of wrinkled colony formation became apparent to the point at which wrinkled colony development ceased or the appropriate data set was collected. Each set of strains for a particular experiment was spotted onto the same plate to account for any minor plate-to-plate variations. Each assay was performed at least 2–3 times, and most were done much more than 3 times. To ensure that cultures spotted at an OD_{600} of 0.2 resulted in the same number of cells inoculated per spot, we evaluated the correlation between cell number and OD. Specifically, we determined the cell number of the pEAH73-containing strains Δ*sypE*, Δ*sypE*Δ*luxU*, Δ*sypE*Δ*luxQ*, and Δ*sypE*Δ*ainR* using cultures normalized to an OD_{600} of 0.2, and found no significant difference in the number of colony-forming units obtained from dilutions of the normalized cultures of these strains.

β-galactosidase assay

Cultures of the reporter strains KV4926 and KV5516 carrying the *sypG* overexpression plasmid pEAH73 were grown in LBS containing Tet at 28°C with shaking. Samples (50 μl) were collected at 12 and 24 hours and 50 μl of Pierce β-galactosidase Assay Reagent (Pierce Biotechnology, Rockford, IL) were added to each sample. Measurements were taken in a microtiter dish using an ELx800 Absorbance Microplate Reader (BioTek, Winooski, VT) with the appropriate settings. As a measure of *syp* transcription, β-galactosidase activity was determined as previously described (Miller, 1972). *P*-values were calculated using the student's t-test.

Supplementary Material

Refer to Web version on PubMed Central for supplementary material.

Acknowledgments

We thank members of the Visick lab and Alan Wolfe for critical reading of the manuscript and helpful comments. We thank Beth Hussa for construction of pEAH90 and Kevin Quirke for construction of the precursors to pVAR29 and pVAR30. We thank Malcolm Winkler and Kyle Wayne for their assistance with phos-tag experiments designed to assess the phosphorylation state of SypG. We also thank our anonymous reviewers and Eric Stabb for the idea that loss of AinR could effect *ainS* expression. This work was funded by NIH Grant GM59690 awarded to K.L.V.

References

Bassler BL, Wright M, Silverman MR. Multiple signalling systems controlling expression of luminescence in *Vibrio harveyi*: sequence and function of genes encoding a second sensory pathway. Mol Microbiol. 1994; 13:273–286. [PubMed: 7984107]

Biondi EG, Skerker JM, Arif M, Prasol MS, Perchuk BS, Laub MT. A phosphorelay system controls stalk biogenesis during cell cycle progression in *Caulobacter crescentus*. Mol Microbiol. 2006; 59:386–401. [PubMed: 16390437]

Boettcher KJ, Ruby EG. Depressed light emission by symbiotic *Vibrio fischeri* of the sepiolid squid *Euprymna scolopes*. J Bacteriol. 1990; 172:3701–3706. [PubMed: 2163384]

Bose JL, Kim U, Bartkowski W, Gunsalus RP, Overley AM, Lyell NL, Visick KL, Stabb EV. Bioluminescence in *Vibrio fischeri* is controlled by the redox-responsive regulator ArcA. Mol Microbiol. 2007; 65:538–553. [PubMed: 17590235]

Bouquin N, Johnson AL, Morgan BA, Johnston LH. Association of the cell cycle transcription factor Mbp1 with the Skn7 response regulator in budding yeast. Mol Biol Cell. 1999; 10:3389–3400. [PubMed: 10512874]

Cao X, Studer SV, Wassarman K, Zhang Y, Ruby EG, Miyashiro T. The novel sigma factor-like regulator RpoQ controls luminescence, chitinase activity, and motility in *Vibrio fischeri*. MBio. 2012; 3:e00285–00211. [PubMed: 22233679]

Croxatto A V, Chalker J, Lauritz J, Jass J, Hardman A, Williams P, Camara M, Milton DL. VanT, a homologue of *Vibrio harveyi* LuxR, regulates serine, metalloprotease, pigment, and biofilm production in *Vibrio anguillarum*. J Bacteriol. 2002; 184:1617–1629. [PubMed: 11872713]

Croxatto A, Pride J, Hardman A, Williams P, Camara M, Milton DL. A distinctive dual-channel quorum-sensing system operates in *Vibrio anguillarum*. Mol Microbiol. 2004; 52:1677–1689. [PubMed: 15186417]

Davis, RW.; Botstein, D.; Roth, JR. Advanced Bacterial Genetics. Cold Spring Harbor Laboratory; Cold Spring Harbor, NY: 1980.

DeLoney CR, Bartley TM, Visick KL. Role for phosphoglucomutase in *Vibrio fischeri-Euprymna scolopes* symbiosis. J Bacteriol. 2002; 184:5121–5129. [PubMed: 12193629]

Domian IJ, Quon KC, Shapiro L. Cell type-specific phosphorylation and proteolysis of a transcriptional regulator controls the G1-to-S transition in a bacterial cell cycle. Cell. 1997; 90:415–424. [PubMed: 9267022]

Egland KA, Greenberg EP. Conversion of the *Vibrio fischeri* transcriptional activator, LuxR, to a repressor. J Bacteriol. 2000; 182:805–811. [PubMed: 10633117]

Enos-Berlage JL, Guvener ZT, Keenan CE, McCarter LL. Genetic determinants of biofilm development of opaque and translucent *Vibrio parahaemolyticus*. Mol Microbiol. 2005; 55:1160–1182. [PubMed: 15686562]

Fidopiastis PM, Miyamoto CM, Jobling MG, Meighen EA, Ruby EG. LitR, a new transcriptional activator in *Vibrio fischeri*, regulates luminescence and symbiotic light organ colonization. Mol Microbiol. 2002; 45:131–143. [PubMed: 12100554]

Freeman JA, Bassler BL. A genetic analysis of the function of LuxO, a two-component response regulator involved in quorum sensing in *Vibrio harveyi*. Mol Microbiol. 1999a; 31:665–677. [PubMed: 10027982]

Freeman JA, Bassler BL. Sequence and function of LuxU: a two-component phosphorelay protein that regulates quorum sensing in *Vibrio harveyi*. J Bacteriol. 1999b; 181:899–906. [PubMed: 9922254]

Gilson L, Kuo A, Dunlap PV. AinS and a new family of autoinducer synthesis proteins. J Bacteriol. 1995; 177:6946–6951. [PubMed: 7592489]

Graf J, Dunlap PV, Ruby EG. Effect of transposon-induced motility mutations on colonization of the host light organ by *Vibrio fischeri*. J Bacteriol. 1994; 176:6986–6991. [PubMed: 7961462]

Gyllborg MC, Sahl JW, Cronin DC 3rd, Rasko DA, Mandel MJ. Draft genome sequence of *Vibrio fischeri* SR5, a strain isolated from the light organ of the Mediterranean squid *Sepiola robusta*. J Bacteriol. 2012; 194:1639. [PubMed: 22374964]

Hammer BK, Bassler BL. Quorum sensing controls biofilm formation in *Vibrio cholerae*. Mol Microbiol. 2003; 50:101–104. [PubMed: 14507367]

Herrero M, de Lorenzo V, Timmis KN. Transposon vectors containing non-antibiotic resistance selection markers for cloning and stable chromosomal insertion of foreign genes in gram-negative bacteria. J Bacteriol. 1990; 172:6557–6567. [PubMed: 2172216]

Hussa EA, Darnell CL, Visick KL. RscS functions upstream of SypG to control the *syp* locus and biofilm formation in *Vibrio fischeri*. J Bacteriol. 2008; 190:4576–4583. [PubMed: 18441059]

Hussa EA, O'Shea TM, Darnell CL, Ruby EG, Visick KL. Two-component response regulators of *Vibrio fischeri*: identification, mutagenesis, and characterization. J Bacteriol. 2007; 189:5825–5838. [PubMed: 17586650]

Iniesta AA, McGrath PT, Reisenauer A, McAdams HH, Shapiro L. A phospho-signaling pathway controls the localization and activity of a protease complex critical for bacterial cell cycle progression. Proc Natl Acad Sci U S A. 2006; 103:10935–10940. [PubMed: 16829582]

Jacobs C, Ausmees N, Cordwell SJ, Shapiro L, Laub MT. Functions of the CckA histidine kinase in *Caulobacter* cell cycle control. Mol Microbiol. 2003; 47:1279–1290. [PubMed: 12603734]

Janiak-Spens F, Sparling DP, West AH. Novel role for an HPt domain in stabilizing the phosphorylated state of a response regulator domain. J Bacteriol. 2000; 182:6673–6678. [PubMed: 11073911]

Kuo A, Callahan SM, Dunlap PV. Modulation of luminescence operon expression by N-octanoyl-L-homoserine lactone in *ainS* mutants of *Vibrio fischeri*. J Bacteriol. 1996; 178:971–976. [PubMed: 8576070]

Le Roux F, Binesse J, Saulnier D, Mazel D. Construction of a *Vibrio splendidus* mutant lacking the metalloprotease gene *vsm* by use of a novel counterselectable suicide vector. Appl Environ Microbiol. 2007; 73:777–784. [PubMed: 17122399]

Lee JH, Rhee JE, Park U, Ju HM, Lee BC, Kim TS, Jeong HS, Choi SH. Identification and functional analysis of *Vibrio vulnificus* SmcR, a novel global regulator. J Microbiol Biotechnol. 2007; 17:325–334. [PubMed: 18051765]

Li S, Ault A, Malone CL, Raitt D, Dean S, Johnston LH, Deschenes RJ, Fassler JS. The yeast histidine protein kinase, Sln1p, mediates phosphotransfer to two response regulators, Ssk1p and Skn7p. EMBO J. 1998; 17:6952–6962. [PubMed: 9843501]

Lupp C, Ruby EG. *Vibrio fischeri* uses two quorum-sensing systems for the regulation of early and late colonization factors. J Bacteriol. 2005; 187:3620–3629. [PubMed: 15901683]

Lupp C, Urbanowski M, Greenberg EP, Ruby EG. The *Vibrio fischeri* quorum-sensing systems *ain* and *lux* sequentially induce luminescence gene expression and are important for persistence in the squid host. Mol Microbiol. 2003; 50:319–331. [PubMed: 14507383]

Lyell NL, Dunn AK, Bose JL, Stabb EV. Bright mutants of *Vibrio fischeri* ES114 reveal conditions and regulators that control bioluminescence and expression of the *lux* operon. J Bacteriol. 2010; 192:5103–5114. [PubMed: 20693328]

Lyell NL, Dunn AK, Bose JL, Vescovi SL, Stabb EV. Effective mutagenesis of *Vibrio fischeri* by using hyperactive mini-Tn*5* derivatives. Appl Environ Microbiol. 2008; 74:7059–7063. [PubMed: 18805998]

Mandel MJ, Wollenberg MS, Stabb EV, Visick KL, Ruby EG. A single regulatory gene is sufficient to alter bacterial host range. Nature. 2009; 458:215–218. [PubMed: 19182778]

McCann J, Stabb EV, Millikan DS, Ruby EG. Population dynamics of *Vibrio fischeri* during infection of *Euprymna scolopes*. Appl Environ Microbiol. 2003; 69:5928–5934. [PubMed: 14532046]

Miller, JH. Experiments in Molecular Genetics. Cold Spring Harbor Laboratory Press; Cold Spring Harbor, NY: 1972.

Milton DL. Quorum sensing in vibrios: complexity for diversification. Int J Med Microbiol. 2006; 296:61–71. [PubMed: 16487746]

Miyamoto CM, Dunlap PV, Ruby EG, Meighen EA. LuxO controls *luxR* expression in *Vibrio harveyi*: evidence for a common regulatory mechanism in *Vibrio*. Mol Microbiol. 2003; 48:537–548. [PubMed: 12675810]

Miyamoto CM, Lin YH, Meighen EA. Control of bioluminescence in *Vibrio fischeri* by the LuxO signal response regulator. Mol Microbiol. 2000; 36:594–607. [PubMed: 10844649]

Miyashiro T, Ruby EG. Shedding light on bioluminescence regulation in *Vibrio fischeri*. Mol Microbiol. 2012; 84:795–806. [PubMed: 22500943]

Miyashiro T, Wollenberg MS, Cao X, Oehlert D, Ruby EG. A single *qrr* gene is necessary and sufficient for LuxO-mediated regulation in *Vibrio fischeri*. Mol Microbiol. 2010; 77:1556–1567. [PubMed: 20662783]

Morgan BA, Bouquin N, Merrill GF, Johnston LH. A yeast transcription factor bypassing the requirement for SBF and DSC1/MBF in budding yeast has homology to bacterial signal transduction proteins. EMBO J. 1995; 14:5679–5689. [PubMed: 8521825]

Morris AR, Darnell CL, Visick KL. Inactivation of a novel response regulator is necessary for biofilm formation and host colonization by *Vibrio fischeri*. Mol Microbiol. 2011; 82:114–130. [PubMed: 21854462]

Neiditch MB, Federle MJ, Miller ST, Bassler BL, Hughson FM. Regulation of LuxPQ receptor activity by the quorum-sensing signal autoinducer-2. Mol Cell. 2005; 18:507–518. [PubMed: 15916958]

Neiditch MB, Federle MJ, Pompeani AJ, Kelly RC, Swem DL, Jeffrey PD, Bassler BL, Hughson FM. Ligand-induced asymmetry in histidine sensor kinase complex regulates quorum sensing. Cell. 2006; 126:1095–1108. [PubMed: 16990134]

Ng WL, Bassler BL. Bacterial quorum-sensing network architectures. Annu Rev Genet. 2009; 43:197–222. [PubMed: 19686078]

Posas F, Saito H. Activation of the yeast SSK2 MAP kinase kinase kinase by the SSK1 two-component response regulator. EMBO J. 1998; 17:1385–1394. [PubMed: 9482735]

Posas F, Wurgler-Murphy SM, Maeda T, Witten EA, Thai TC, Saito H. Yeast HOG1 MAP kinase cascade is regulated by a multistep phosphorelay mechanism in the SLN1-YPD1-SSK1 “two-component” osmosensor. Cell. 1996; 86:865–875. [PubMed: 8808622]

Quon KC, Yang B, Domian IJ, Shapiro L, Marczynski GT. Negative control of bacterial DNA replication by a cell cycle regulatory protein that binds at the chromosome origin. Proc Natl Acad Sci U S A. 1998; 95:120–125. [PubMed: 9419339]

Sanders DA, Gillece-Castro BL, Burlingame AL, Koshland DE Jr. Phosphorylation site of NtrC, a protein phosphatase whose covalent intermediate activates transcription. J Bacteriol. 1992; 174:5117–5122. [PubMed: 1321122]

Sanders DA, Gillece-Castro BL, Stock AM, Burlingame AL, Koshland DE Jr. Identification of the site of phosphorylation of the chemotaxis response regulator protein, CheY. J Biol Chem. 1989; 264:21770–21778. [PubMed: 2689446]

Shibata S, Visick KL. Sensor kinase RscS induces the production of antigenically distinct outer membrane vesicles that depend on the symbiosis polysaccharide locus in *Vibrio fischeri*. J Bacteriol. 2012; 194:185–194. [PubMed: 22020639]

Shikuma NJ, Fong JC, Odell LS, Perchuk BS, Laub MT, Yildiz FH. Overexpression of VpsS, a hybrid sensor kinase, enhances biofilm formation in *Vibrio cholerae*. J Bacteriol. 2009; 191:5147–5158. [PubMed: 19525342]

Sitnikov DM, Schineller JB, Baldwin TO. Transcriptional regulation of bioluminesence genes from *Vibrio fischeri*. Mol Microbiol. 1995; 17:801–812. [PubMed: 8596430]

Stabb, E.; Schaefer, A.; Bose, JL.; Ruby, EG. Quorum Signalling and Symbiosis in the Marine Luminous Bacterium *Vibrio fischeri*. In: Winans, SC.; Bassler, BL., editors. Chemical Communication among Bacteria. Washington, DC: ASM Press; 2008. p. 233-250.

Stabb EV, Ruby EG. RP4-based plasmids for conjugation between *Escherichia coli* and members of the *Vibrionaceae*. Methods Enzymol. 2002; 358:413–426. [PubMed: 12474404]

Stevens AM, Dolan KM, Greenberg EP. Synergistic binding of the *Vibrio fischeri* LuxR transcriptional activator domain and RNA polymerase to the *lux* promoter region. Proc Natl Acad Sci U S A. 1994; 91:12619–12623. [PubMed: 7809088]

Stock AM V, Robinson L, Goudreau PN. Two-component signal transduction. Annu Rev Biochem. 2000; 69:183–215. [PubMed: 10966457]

Studer SV, Mandel MJ, Ruby EG. AinS quorum sensing regulates the *Vibrio fischeri* acetate switch. J Bacteriol. 2008; 190:5915–5923. [PubMed: 18487321]

Visick KL. Layers of signaling in a bacterium-host association. J Bacteriol. 2005; 187:3603–3606. [PubMed: 15901681]

Visick KL, Skoufos LM. Two-component sensor required for normal symbiotic colonization of *Euprymna scolopes* by *Vibrio fischeri*. J Bacteriol. 2001; 183:835–842. [PubMed: 11208780]

Weber B, Lindell K, El Qaidi S, Hjerde E, Willassen NP, Milton DL. The phosphotransferase VanU represses expression of four *qrr* genes antagonizing VanO-mediated quorum-sensing regulation in *Vibrio anguillarum*. Microbiology. 2011; 157:3324–3339. [PubMed: 21948044]

West AH, Stock AM. Histidine kinases and response regulator proteins in two-component signaling systems. Trends Biochem Sci. 2001; 26:369–376. [PubMed: 11406410]

Yip ES, Geszvain K, DeLoney-Marino CR, Visick KL. The symbiosis regulator *rscS* controls the *syp* gene locus, biofilm formation and symbiotic aggregation by *Vibrio fischeri*. Mol Microbiol. 2006; 62:1586–1600. [PubMed: 17087775]

Yip ES, Grublesky BT, Hussa EA, Visick KL. A novel, conserved cluster of genes promotes symbiotic colonization and sigma(54)-dependent biofilm formation by *Vibrio fischeri*. Mol Microbiol. 2005; 57:1485–1498. [PubMed: 16102015]

Zhang Y, Qiu Y, Tan Y, Guo Z, Yang R, Zhou D. Transcriptional Regulation of *opaR*, *qrr2-4* and *aphA* by the Master Quorum-Sensing Regulator OpaR in *Vibrio parahaemolyticus*. PLoS One. 2012; 7:e34622. [PubMed: 22506036]

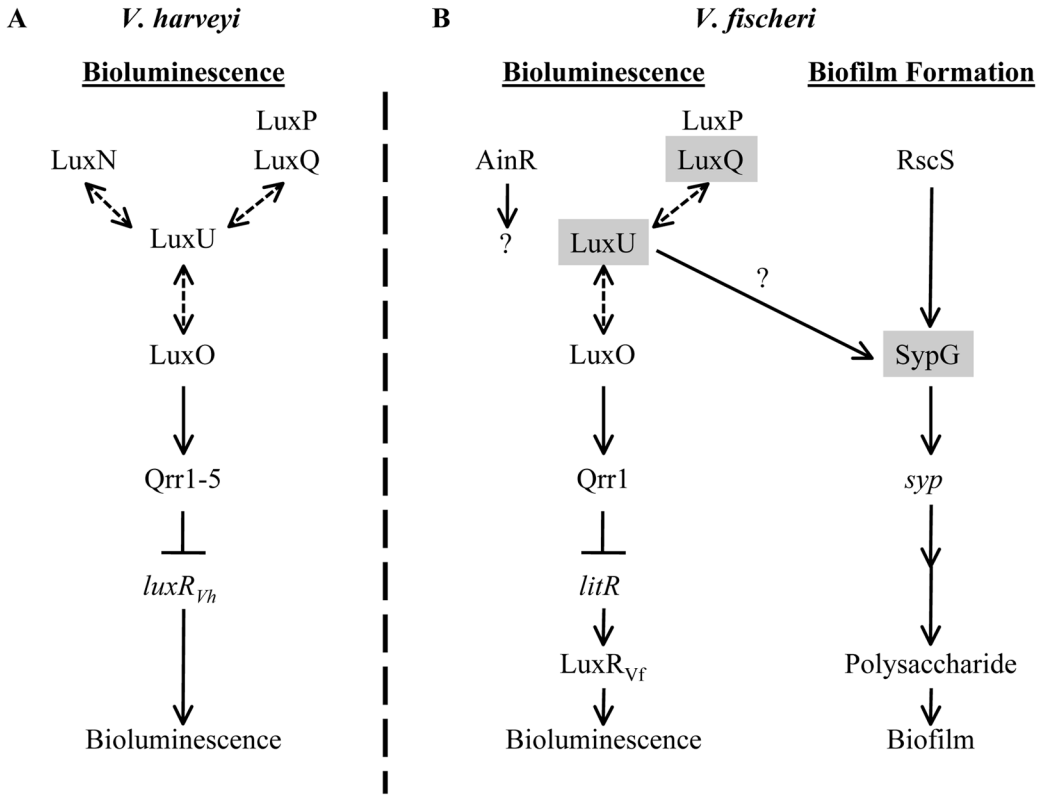

Fig. 1. Models for the regulation by the Lux and Syp pathways

(A) In *V. harveyi*, bioluminescence is regulated by the Lux phosphorelay, composed of the sensor kinases (SKs) LuxQ (which interacts with the periplasmic protein LuxP), LuxN, and CqsS (not depicted), the phosphotransferase LuxU, and the response regulator (RR) LuxO. Phosphoryl-transfer (dashed, double-sided arrows) occurs between the SKs, LuxU, and LuxO. Under low cell density conditions, LuxO is phosphorylated by the kinase activity of the SKs and activates transcription of the *qrr* sRNAs, which bind to the transcript of *luxR*$_{VH}$ and prevent its translation. Without LuxR$_{VH}$, the *lux* operon (not depicted) is not expressed and light (bioluminescence) is not produced. At high cell densities, LuxO is dephosphorylated by the phosphatase activity of the SKs, leading to subsequent production of LuxR$_{VH}$ and bioluminescence. Autoinducers (AIs) or the AI synthases (LuxM, LuxS, or CqsA) are not depicted for simplicity.

(B) In *V. fischeri*, the Lux phosphorelay functions in largely the same manner to regulate bioluminescence, with homologs of LuxP, LuxQ, LuxU, and LuxO, but not CqsS or LuxN; *V. fischeri* encodes another putative SK, AinR. Additionally, *V. fischeri* uses the LuxR$_{VH}$ homolog, LitR, to activate transcription of LuxR$_{VF}$ (not similar to LuxR$_{VH}$), which promotes transcription of the *lux* operon (when bound to the AI produced by LuxI) (not depicted), leading to subsequent light production (bioluminescence). Regulators shaded in gray indicate those found in this study to be involved in biofilm formation. RscS is an SK known to control biofilm formation. Phosphorylation of the RR SypG is predicted to activate transcription of the *syp* locus, which encodes proteins thought to regulate, produce, and transport a polysaccharide necessary for biofilm formation. The specific activity of LuxU in activating biofilm formation is unknown, but it appears from the current study to work at or above the level of *syp* transcription, likely at the level of SypG activation (indicated by a question mark). This figure is adapted from (Visick, 2005).

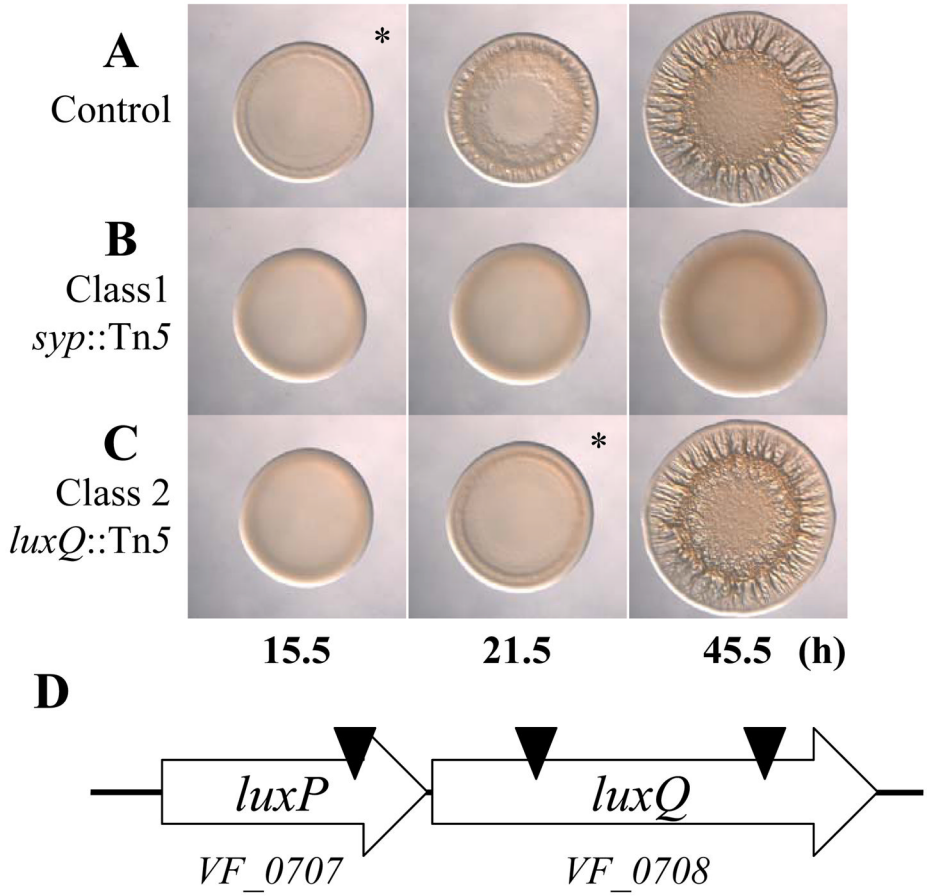

Fig. 2.

Transposon mutagenesis reveals other regulators of biofilm formation in *V. fischeri*. (A–C). Time-course assays of wrinkled colony formation induced by *sypG* overexpression using plasmid pEAH73. Cultures were spotted onto LBS medium containing Tet and incubated at 28°C. Wrinkled colony formation was monitored up to 45.5 h post-spotting for the following strains: Δ*sypE* control (pEAH73/KV3299) (A), a representative class 1 mutant (pEAH73/KV5872; *syp*::Tn*5* Δ*sypE*) (B), and a representative class 2 mutant (pEAH73/KV4431; *luxQ*::Tn*5* Δ*sypE*) (C). An * indicates the time at which wrinkled colony formation was apparent, typically identified by the presence of ridges around the outer edge of the spot. Data are representative of at least three independent experiments. (D). A graphical depiction of the predicted *luxPQ* genes (block arrows) and Tn insertion sites (black triangles). There are 2 bp between the predicted translational stop site of *luxP* and the predicted translational start site of *luxQ*.

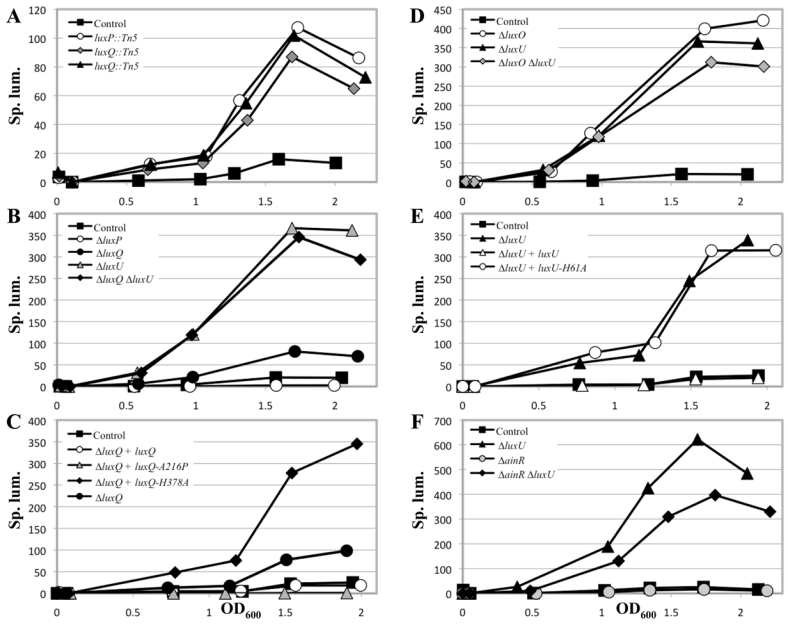

Fig. 3.

Luminescence of *lux* mutants in culture. Cultures were grown in SWTO and incubated at 24°C with vigorous shaking. Luminescence and OD_{600} were measured over time until maximum luminescence was achieved (between OD_{600} 1.5 and 2). All data are plotted as specific luminescence (Sp. lum.; relative luminescence divided by OD_{600}) versus OD_{600} and are representative of at least 3 independent experiments.

A. Δ*sypE* control (black squares; KV3299), *luxP*::Tn*5* Δ*sypE* (white circles; KV4430), *luxQ*::Tn*5* Δ*sypE* (grey diamonds; KV4431), *luxQ*::Tn*5* Δ*sypE* (black triangles; KV4432)

B. Δ*sypE* control (black squares; KV3299), Δ*luxP* Δ*sypE* (white circles; KV5347), Δ*luxQ* Δ*sypE* (black circles; KV5394), Δ*luxU* Δ*sypE* (grey triangles; KV4830), Δ*luxQ* Δ*luxU* Δ*sypE* (black diamonds; KV6008)

C. Δ*sypE attTn7::erm* control (black squares; KV4390), Δ*luxQ* Δ*sypE attTn7::erm* (black circles; KV5973), Δ*luxQ* Δ*sypE attTn7::luxQ-FLAG* (white circles; KV5902), Δ*luxQ* Δ*sypE attTn7::luxQ-A216P-FLAG* (grey triangles; KV5904), Δ*luxQ* Δ*sypE attTn7::luxQ-H378A-FLAG* (black diamonds; KV5903)

D. Δ*sypE* control (black squares; KV3299), Δ*luxO* Δ*sypE* (white circles; KV5468), Δ*luxU* Δ*sypE* (black triangles; KV4830), Δ*luxO* Δ*luxU* Δ*sypE* (grey diamonds; KV5472)

E. Δ*sypE attTn7::erm* control (black squares; KV4390), Δ*luxU* Δ*sypE attTn7::erm* (black triangles; KV5974), Δ*luxU* Δ*sypE attTn7::luxU-FLAG* (white triangles; KV5905), Δ*luxU* Δ*sypE attTn7::luxU-H61A-FLAG* (white circles; KV5906)

F. Δ*sypE* control (black squares; KV3299), Δ*ainR* Δ*sypE* (grey circles; KV6169), Δ*luxU* Δ*sypE* (black triangles; KV4830), Δ*ainR* Δ*luxU* Δ*sypE* (black diamonds; KV6259)

The data for KV3299 in panel B are the same as that shown in panel D. The data for KV4390 in panel C are the same as that shown in panel E.

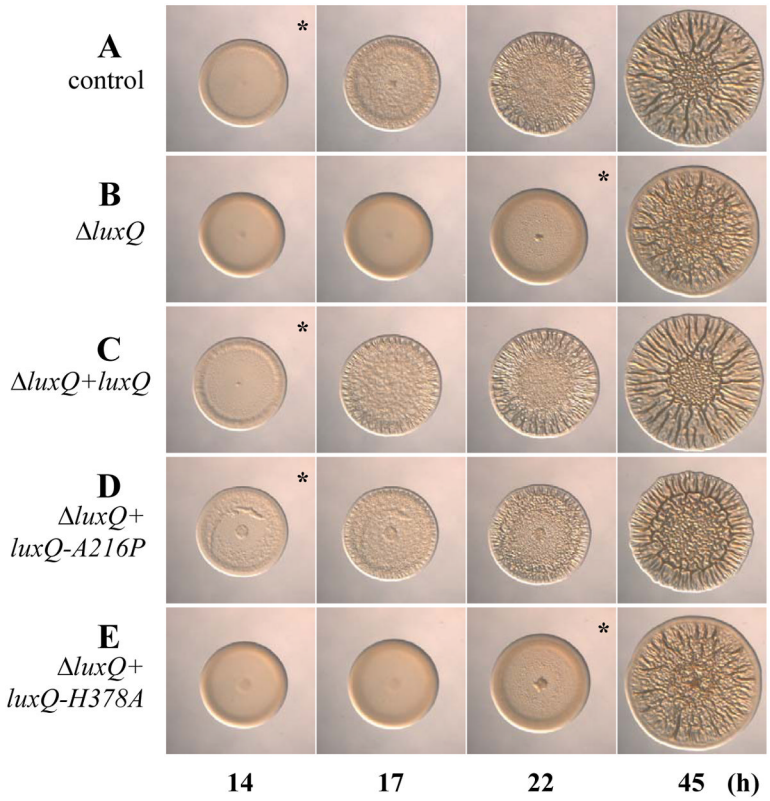

Fig. 4.

The effect of *luxQ* point mutations on biofilm formation. Time-course assays of wrinkled colony formation induced by *sypG* overexpression using plasmid pEAH73. Cultures were spotted onto LBS medium containing Tet and incubated at 28°C. Wrinkled colony formation was monitored up to 45 h post-spotting for the following strains: Δ*sypE att*Tn*7::erm* control (pEAH73/KV4390) (A), Δ*luxQ* Δ*sypE att*Tn*7::erm* (pEAH73/KV5973) (B), Δ*luxQ* Δ*sypE att*Tn*7::luxQ-FLAG* (pEAH73/KV5902) (C), Δ*luxQ* Δ*sypE att*Tn*7::luxQ-A216P-FLAG* (pEAH73/KV5904) (D), and Δ*luxQ* Δ*sypE att*Tn*7::luxQ-H378A-FLAG* (pEAH73/KV5903) (E). An * indicates the time at which wrinkled colony formation was apparent, typically identified by the presence of ridges around the outer edge of the spot. Data are representative of at least three independent experiments.

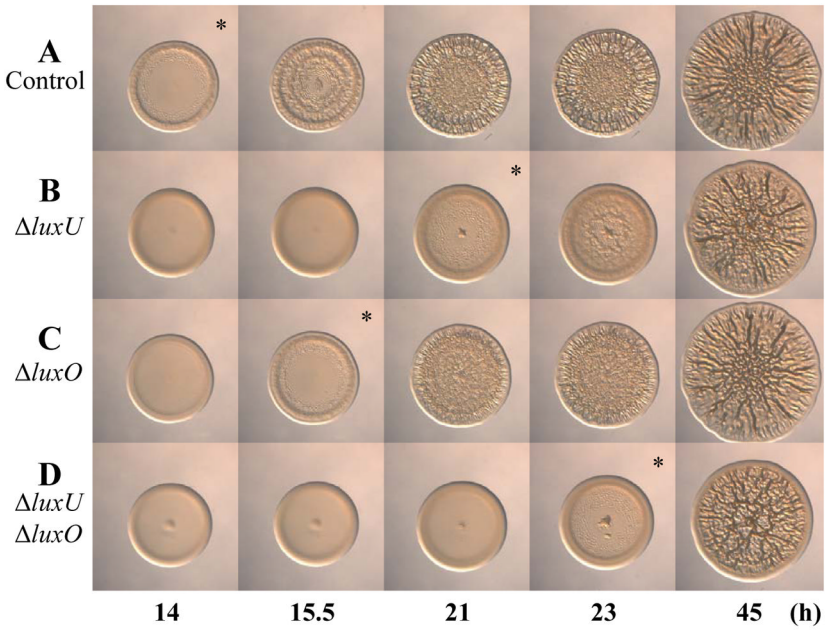

Fig. 5.

Wrinkled colony formation by *luxU* and *luxO* mutants. Time-course assays of wrinkled colony formation induced by *sypG* overexpression using plasmid pEAH73. Cultures were spotted onto LBS medium containing Tet and incubated at 28 C. Wrinkled colony formation was monitored up to 45 h post-spotting for the following strains: Δ*sypE* control (pEAH73/KV3299) (A), Δ*luxU* Δ*sypE* (pEAH73/KV4830) (B), Δ*luxO* Δ*sypE* (pEAH73/KV5468) (C), and Δ*luxO* Δ*luxU* Δ*sypE* (pEAH73/KV5472) (D). An * indicates the time at which wrinkled colony formation was apparent, typically identified by the presence of ridges around the outer edge of the spot. Data are representative of at least three independent experiments.

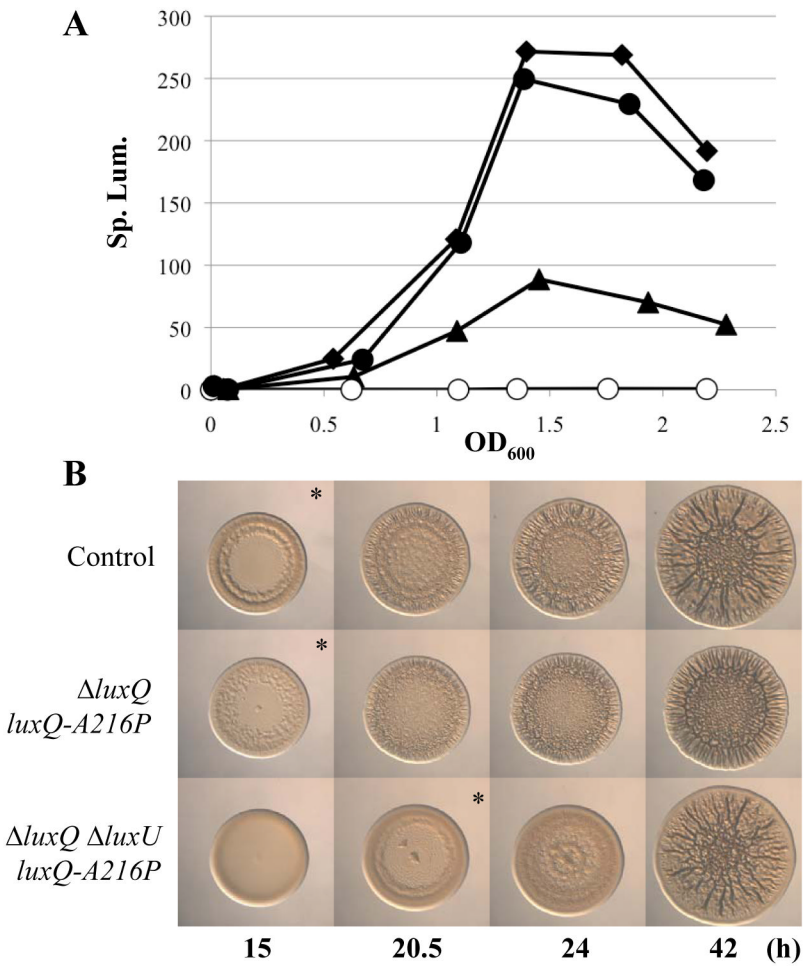

Fig. 6. Luminescence and wrinkled colony formation by *luxQ* and *luxU* mutants

(A) Luminescence of *lux* mutants in culture. Cultures were grown in SWTO and incubated at 24°C with vigorous shaking. Luminescence and OD_{600} were measured over time until maximum luminescence was achieved (between OD_{600} 1.5 and 2) for the following strains: Δ*luxQ attTn7::erm* control (black triangles; KV5973), Δ*luxU* Δ*sypE attTn7::erm* (black diamonds; KV5974), Δ*luxQ* Δ*sypE attTn7::luxQ-A216P-FLAG* (white circles; KV5904), and Δ*luxQ* Δ*luxU* Δ*sypE attTn7::luxQ-A216P-FLAG* (black circles; KV6054). All data are plotted as specific luminescence (Sp. lum.; relative luminescence divided by OD_{600}) versus OD_{600} and are representative of at least 3 independent experiments.

(B) Time-course assays of wrinkled colony formation induced by *sypG* overexpression using plasmid pEAH73. Cultures were spotted onto LBS medium containing Tet and incubated at 28°C. Wrinkled colony formation was monitored up to 42 h post-spotting for the following strains: Δ*sypE attTn7::erm* control (pEAH73/KV4390), Δ*luxQ* Δ*sypE attTn7::luxQ-A216P-FLAG* (pEAH73/KV5904), and Δ*luxQ* Δ*luxU sypE attTn7::luxQ-A216P-FLAG* (pEAH73/KV6054). An * indicates the time at which wrinkled colony formation was apparent, typically identified by the presence of ridges around the outer edge of the spot. Data are representative of at least three independent experiments.

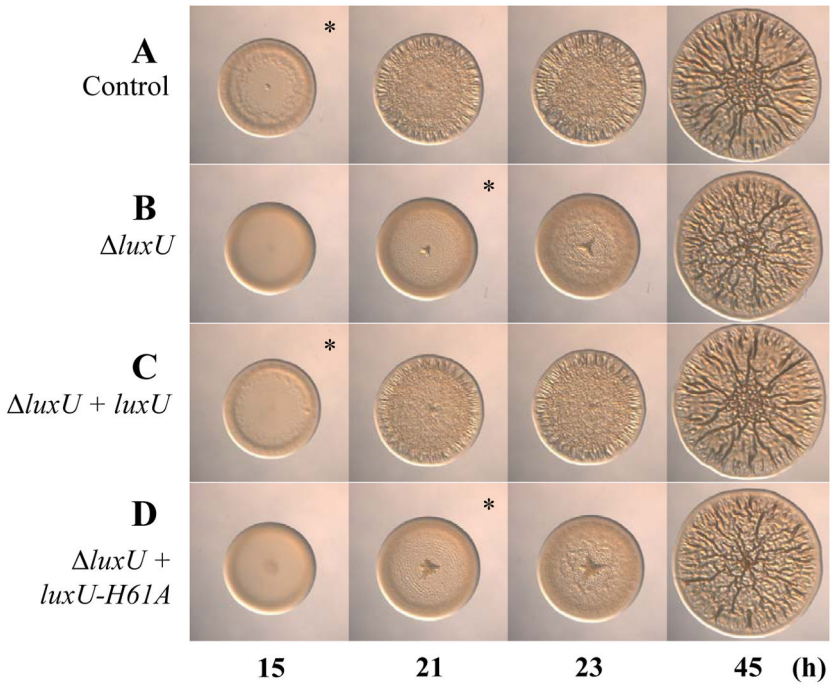

Fig. 7.

Wrinkled colony formation by complemented Δ*luxU* mutants. Time-course assays of wrinkled colony formation induced by *sypG* overexpression using plasmid pEAH73. Cultures were spotted onto LBS medium containing Tet and incubated at 28°C. Wrinkled colony formation was monitored up to 45 h post-spotting for the following strains: Δ*sypE attTn7::erm* control (pEAH73/KV4390) (A), Δ*luxU* Δ*sypE attTn7::erm* (pEAH73/KV5974) (B), Δ*luxU* Δ*sypE attTn7::luxU-FLAG* (pEAH73/KV5905) (C), and Δ*luxU* Δ*sypE attTn7::luxU-H61A-FLAG* (pEAH73/KV5906) (D). An * indicates the time at which wrinkled colony formation was apparent, typically identified by the presence of ridges around the outer edge of the spot. Data are representative of at least three independent experiments.

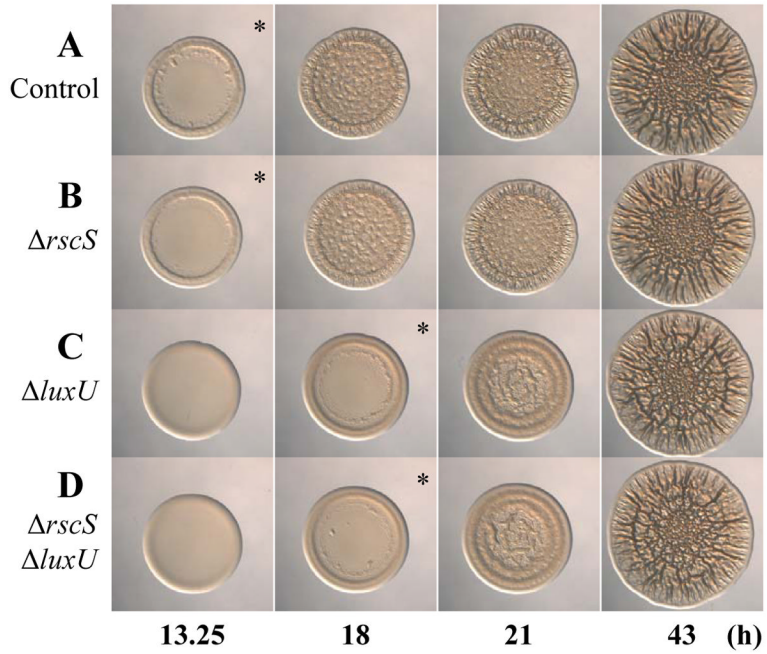

Fig. 8.

Wrinkled colony formation by *luxU* and *rscS* mutants. Time-course assays of wrinkled colony formation induced by *sypG* overexpression using plasmid pEAH73. Cultures were spotted onto LBS medium containing Tet and incubated at 28°C. Wrinkled colony formation was monitored up to 43 h post-spotting for the following strains: Δ*sypE* control (pEAH73/KV3299) (A), Δ*rscS* Δ*sypE* (pEAH73/KV6268) (B), Δ*luxU* Δ*sypE* (pEAH73/KV4830) (C), and Δ*rscS* Δ*luxU* Δ*sypE* (pEAH73/KV6269) (D). An * indicates the time at which initiation of wrinkled colony formation was apparent, typically identified by the presence of ridges around the outer edge of the spot. Data are representative of at least three independent experiments.

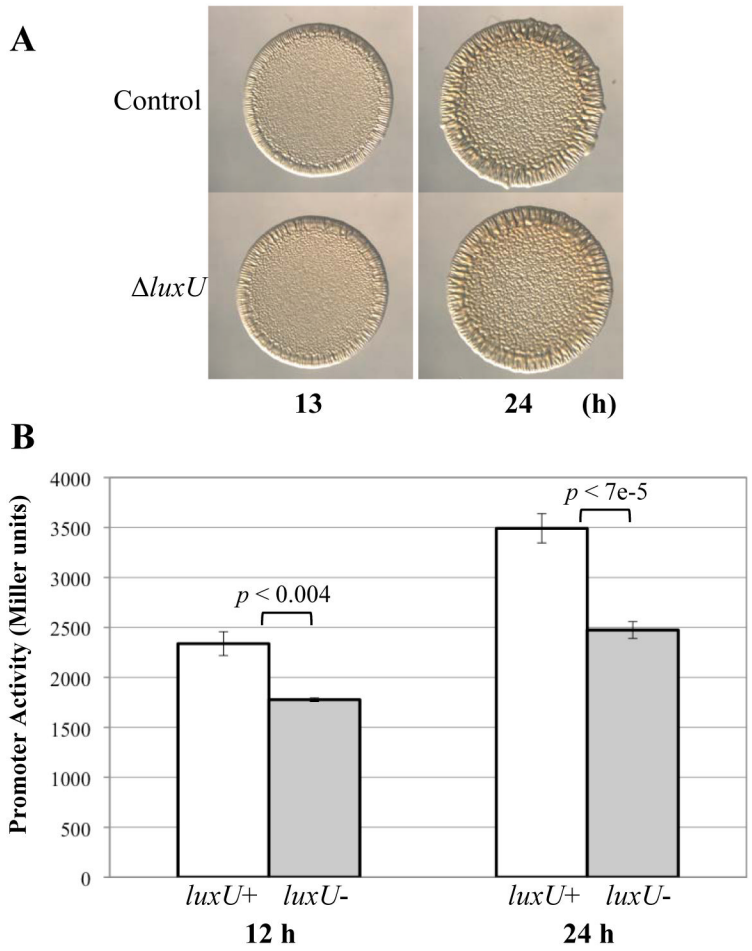

Fig. 9. The role of LuxU in *syp* activation

(A) Time-course assays of wrinkled colony formation induced by *sypG-D53E* overexpression using plasmid pKV276. Cultures were spotted onto LBS medium containing Tet and incubated at 28°C. Wrinkled colony formation was monitored up to 24 h post-spotting for the following strains: Δ*sypE* control (pKV276/KV3299) and Δ*luxU* Δ*sypE* (pKV276/KV4830). Data are representative of at least three independent experiments. (B) SypG-induced *syp* transcription from P_{sypA}-*lacZ* reporter strains. Cultures of *sypG* overexpressing strains Δ*sypE attTn7*::P_{sypA}-*lacZ* (white bars; pEAH73/KV4926) and Δ*luxU* Δ*sypE attTn7*::P_{sypA}-*lacZ* (grey bars; pEAH73/KV5516) were inoculated in LBS containing Tet and grown at 28°C with shaking. Samples were collected at 12 and 24 h and assessed for β-galactosidase activity (in Miller units) as a measure of promoter activity. All experiments were performed in triplicate. Data are a combination of two independent experiments with error bars representing the standard error. The *P*-value refers to the variation between the two samples as indicated by the brackets.

Table 1

V. fischeri strains used in this study.

Strains	Relevant Genotype	Reference
ES114	wild-type	(Boettcher & Ruby, 1990)
KV3299	Δ*sypE*	(Hussa *et al.*, 2008)
KV4390	Δ*sypE attTn7::erm*	(Morris *et al.*, 2011)
KV4430	*luxP*::Tn*5* Δ*sypE*	This study
KV4431	*luxQ*::Tn*5* Δ*sypE*	This study
KV4432	*luxQ*::Tn*5* Δ*sypE*	This study
KV4830	Δ*luxU* Δ*sypE*	This study
KV4926	Δ*sypE attTn7*::P_{sypA}-*lacZ* (Erm^r)	This study
KV5347	Δ*luxP* Δ*sypE*	This study
KV5394	Δ*luxQ* Δ*sypE*	This study
KV5468	Δ*luxO* Δ*sypE*	This study
KV5472	Δ*luxO* Δ*luxU* Δ*sypE*	This study
KV5516	Δ*luxU* Δ*sypE attTn7*::P_{sypA}-*lacZ* (Erm^r)	This study
KV5872	*syp*::Tn*5* Δ*sypE*	This study
KV5902	Δ*luxQ* Δ*sypE attTn7::luxQ-FLAG*	This study
KV5903	Δ*luxQ* Δ*sypE attTn7::luxQ-H378A-FLAG*	This study
KV5904	Δ*luxQ* Δ*sypE attTn7::luxQ-A216P-FLAG*	This study
KV5905	Δ*luxU* Δ*sypE attTn7::luxU-FLAG*	This study
KV5906	Δ*luxU* Δ*sypE attTn7::luxU-H61A-FLAG*	This study
KV5973	Δ*luxQ* Δ*sypE attTn7::erm*	This study
KV5974	Δ*luxU* Δ*sypE attTn7::erm*	This study
KV6008	Δ*luxQ*Δ *luxU* Δ*sypE*	This study
KV6054	Δ*luxQ* Δ*luxU* Δ*sypE attTn7::luxQ-A216P-FLAG*	This study
KV6196	Δ*ainR* Δ*sypE*	This study
KV6259	Δ*ainR* Δ*luxU* Δ*sypE*	This study
KV6268	Δ*rscS* Δ*sypE*	This study
KV6269	Δ*rscS* Δ*luxU* Δ*sypE*	This study

Table 2

Plasmids used in this study.

Plasmids		
pEAH73	pKV69 carrying wild-type *sypG*; Cm^r Tet^r	(Hussa *et al.*, 2008)
pEAH90	pEVS107 the P_{sypA} promoter region (generated with primers 714 and 782) upstream of promoterless *lacZ*	This study
pEVS104	Conjugal helper plasmid (*tra trb*); Kan^r	(Stabb & Ruby, 2002)
pEVS107	Mini-Tn7 delivery plasmid; *oriR6K*, *mob*; Kan^r, Erm^r	(McCann *et al.*, 2003)
pJET1.2	Commercial cloning vector; Ap^r	Fermentas
pKV69	Mobilizable vector; Cm^r Tet^r	(Visick & Skoufos, 2001)
pKV276	pEAH73 with D53E mutation in *sypG*; Cm^r Tet^r	(Hussa *et al.*, 2008)
pKV363	Mobilizable suicide vector; Cm^r	(Shibata & Visick, 2012)
pSW7848	Mobilizable suicide vector; Cm^r	Marie-Eve Val
pVAR17	pSW7848 containing 2 kb sequence flanking *sypE* derived from pCLD19	(Hussa et al., 2008) and this study
pVAR18	pSW7848 containing 3.3 kb sequence flanking *luxU* using primers 995, 996, 1017, and 1018	This study
pVAR29	pKV363 containing 850 bp sequencing flanking *luxQ* using primers 1286, 1287, 1288, 1304	This study
pVAR30	pKV363 containing 1.1 kb sequence flanking *luxP* using primers 1282, 1283, 1284, and 1303	This study
pVAR36	pKV363 containing 1.1 kb sequence flanking *luxO* using primers 1319, 1320, 1344, and 1345	This study
pVAR37	pKV363 containing 1.1 kb sequence flanking *luxO* and *luxU* using primers 1319, 1321, 1344, and 1346	This study
pVAR52	pEVS107 with P_{lacZ} containing 2.3 kb *luxQ*-FLAG allele using primers 1314 and 1437	This study
pVAR53	pEVS107 with P_{lacZ} containing 2.3 kb *luxQ-A216P*-FLAG allele using primers 849 and 1425	This study
pVAR54	pEVS107 with P_{lacZ} containing 2.3 kb *luxQ-H378A*-FLAG allele using primers 849 and 1426	This study
pVAR55	pEVS107 with P_{lacZ} containing 400 bp *luxU*-FLAG allele using primers 1312 and 1422	This study
pVAR56	pEVS107 with P_{lacZ} containing 400 bp *luxU-H61A*-FLAG allele using primers 849 and 1427	This study
pVAR62	pKV363 containing 1.1 kb sequence flanking *ainR* using primers 1323 and pr_NL35 (Lyell *et al.*, 2010)	This study